J. Membrane Biol. 152, 13–23 (1996)

The Journal of
Membrane
Biology

Calcium-dependent Modulation of the Agonist Affinity of the Mammalian Olfactory Cyclic Nucleotide-gated Channel by Calmodulin and a Novel Endogenous Factor

S. Balasubramanian,[1] **J.W. Lynch,**[2] **P.H. Barry**[1]

[1]School of Physiology and Pharmacology, University of New South Wales, Sydney 2052, Australia, [2]Neurobiology Division, Garvan Institute of Medical Research, Darlinghurst, Sydney 2010, Australia

Received: 26 December 1995/Revised: 14 March 1996

Abstract. The calcium-dependent modulation of the affinity of the cyclic nucleotide-gated (CNG) channels for adenosine 3′,5′-cyclic monophosphate (cAMP) was studied in enzymatically dissociated rat olfactory receptor neurons, by recording macroscopic cAMP-activated currents from inside-out patches excised from their dendritic knobs. Upon intracellular addition of 0.2 mM Ca^{2+} (0.2 Ca) the concentration of cAMP required for the activation of half-maximal current (EC_{50}) was reversibly increased from 3 μM to about 30 μM. This Ca^{2+}-induced affinity shift was insensitive to the calmodulin antagonist, mastoparan, was abolished irreversibly by a 2-min exposure to 3 mM Mg^{2+} + 2 mM EGTA (Mg + EGTA), and was not restored by the application of calmodulin (CAM). Addition of CAM plus 0.2 mM Ca^{2+} (0.2 Ca + CAM), further reversibly shifted the cAMP affinity from 30 μM to about 200 μM. This affinity shift was not affected by Mg + EGTA exposure, but was reversed by mastoparan. Thus, the former Ca^{2+}-only effect must be mediated by an unknown endogenous factor, distinct from CAM. Removal of this factor also increased the affinity of the channel for CAM. The affinity shift induced by Ca^{2+}-only was maintained in the presence of the nonhydrolyzable cAMP analogue, 8-bromo-cAMP and the phosphatase inhibitor, microcystin-LR, ruling out modulation by phosphodiesterases or phosphatases. Our results indicate that the olfactory CNG channels are modulated by an as yet unidentified factor distinct from CAM.

Key words: Olfactory receptor neuron — CNG channel — Cyclic AMP — Ca^{2+} — Calmodulin

Correspondence to: P.H. Barry

Introduction

Upon stimulation by odorants, the olfactory receptor neurons (ORNs) produce the intracellular second messengers, adenosine 3′,5′-cyclic monophosphate (cAMP) and inositol 1,4,5,-trisphosphate (IP_3) (Boekhoff et al., 1990; Reed, 1992; Ronnet et al., 1993) to initiate the signal transduction cascade. The initial steps of olfactory signal transduction occur in the ciliary and dendritic knob membranes of the ORNs (Lowe & Gold, 1991). Direct activation of the cyclic nucleotide-gated (CNG) cationic channels (Nakamura & Gold, 1987) causes an influx of cations. These channels, which are highly permeable to calcium (Frings et al., 1995), initiate the spike-generating receptor potential by either directly depolarizing the cell or by activating a calcium-sensitive chloride conductance (Kurahashi & Yau, 1992; Kleene, 1993). Although the steps involved in the initiation of the odorant response have been studied in detail, much less is known about the termination and adaptation of the response.

Desensitization of the olfactory signal is mediated by Ca^{2+} entry through CNG channels (Kurahashi & Shibuya, 1990). One of the mechanisms underlying this effect is a Ca^{2+}-induced reduction in the affinity of these channels for cAMP (Kramer & Siegelbaum, 1992; Lynch & Lindemann, 1994; Chen & Yau, 1994), which is mediated at least in part by a calcium-activated calmodulin (CAM) binding site on the olfactory CNG channel α subunit (Liu et al., 1994). To date, there is no clear evidence that the cyclic nucleotide affinity of these channels is modulated by any other factor. However, in the homologous photoreceptor cGMP-gated channel, several mechanisms appear to contribute to the modulation of agonist affinity (Gordon, Brautigan & Zimmerman, 1992; Hsu & Molday, 1993; Nakatani, Koutalos & Yau, 1995; Gordon, Downing-Park & Zimmerman, 1995).

In this study, we have examined the mechanisms underlying the Ca^{2+}-mediated reduction in the cyclic nucleotide affinity of native rat olfactory CNG channels in order to determine whether cAMP affinity reduction occurs only through activation of CAM or whether it also occurs by other mechanisms. This investigation was performed on excised membrane patches from the dendritic knob of rat ORNs. Preliminary results of this work have been published in abstract form (Balasubramanian, Lynch & Barry, 1995*a*).

Materials and Methods

Cell Preparation

Enzymatically dissociated olfactory receptor neurons were obtained from olfactory epithelial tissue lining the septum and the turbinates of the nasal cavity of adult female Wistar rats killed quickly by CO_2 inhalation. Cell dissociation and isolation techniques were basically the same as described previously (e.g., Lynch & Barry, 1991; Balasubramanian et al., 1995*b*). Briefly, olfactory receptor neurons were dissociated by incubating the olfactory epithelial tissue pieces for 27 min at 37°C in divalent cation-free Dulbecco's phosphate buffered saline (DPBS) containing 0.2 mg/ml of trypsin (Calbiochem, La Jolla, CA). The dissociation was terminated by removing the dissociation solution and replacing it with 10 ml of General Mammalian Ringer's solution (GMR) to which 0.1 mg trypsin inhibitor (Calbiochem, La Jolla, CA) had been added. After trituration with a wide-bored pipette, about 2 ml of the supernatant containing isolated cells were placed in a glass-bottomed chamber. The cells were allowed to settle for about 30 min and were then continuously superfused by GMR, containing (in mM): NaCl 140, KCl 5, $CaCl_2$ 2, $MgCl_2$ 1, Glucose 10 and HEPES 10 (pH 7.4 with NaOH). Several types of cells were present in the preparation but the olfactory receptor neurons were identified by their characteristic bipolar morphology with a spherical or ovoid soma, an axon and a single dendrite arising from the soma and ending in the olfactory knob, which bears several fine cilia. The dissection and the experiments were performed at room temperature (20–22°C).

Solutions and Perfusion System

The ionic composition of the solution filling the patch pipette was the same in all experiments and contained (in mM): NaCl 140, EGTA 10, NaOH 25, and HEPES 10 titrated to pH 7.4 with NaOH. The control (zero calcium) solution used to bathe the cytoplasmic side of the membrane patch contained (in mM): NaCl 155, NaOH 10, EGTA 2, HEPES 10, with pH titrated to 7.4 with NaOH. The free Ca^{2+} concentration of these solutions was calculated to be less than 1 nM (Balasubramanian et al., 1995*b*). The low extracellular Ca^{2+} concentration was used to avoid complications caused by its permeation through the channels. Sodium salts of the agonist cAMP or 8-Bromo-cAMP were added in appropriate concentrations to this zero calcium solution. To study the effects of calcium ions, various chemicals and the chloride salts of Ca^{2+} were added to a solution which had the same composition as the control solution (zero calcium) but with no EGTA. In some experiments, the chloride salt of Mg^{2+} was added to the control (zero calcium) solution containing 2 mM EGTA. The following chemicals were used: sodium salts of cAMP and 8-bromo-cAMP, mastoparan (catalog no. M5280) and calmodulin (all from Sigma Chemical, St. Louis, MO) and microcystin-LR (Calbiochem, La Jolla, CA). Stock solutions of appropriate concentrations of these chemicals were prepared by dissolving them in distilled water and storing in aliquots at −20°C.

For simplicity, the zero divalent ion control solution will be referred to as '0Ca', the solution with 0.2 mM $Ca^{2+}$and without EGTA will be referred to as '0.2 Ca', the standard 0.2 Ca solution with 470 nM calmodulin solution as '0.2 Ca + CAM', and the 120 nM CAM solution (*See* below and Fig. 5*A* and *B*) as '0.2 Ca + low CAM'.

A multibarrel perfusion system was set up to enable solutions to be changed effectively and rapidly across the membrane patch. The cells were stored in a separate compartment and on-cell patches on the dendritic knobs formed amidst the cilia in this compartment, (Fig. 1*A* and *B*), before excised inside-out configurations were produced by brief exposure to the air-solution interface. The patch of membrane spanning the patch pipette was moved through a narrow channel of solution to a separate compartment equipped with up to ten perfusion tubes, and visually positioned in front of the perfusion tubes through which the control and test solutions flowed (*see* Fig. 1*B*).

Electrophysiological Recording

Membrane currents through the CNG channels were studied in excised inside-out patches from the dendritic knobs of isolated olfactory receptor neurons using standard patch clamp techniques (Hamill et al., 1981). Fire-polished patch pipettes with a tip diameter of about 0.2 μm and resistance of 10–15 MΩ were used to obtain gigaohm seals on the membrane. Channels were activated by the addition of the sodium salt of cAMP or 8-bromo-cAMP. Currents were measured using an Axopatch-1D patch-clamp amplifier (Axon Instruments, Foster City, CA). The current signal was filtered at 2 kHz and digitized at a sampling interval of 0.1 msec, monitored online and stored on an IBM-compatible 80486 computer running pCLAMP software (V.6.0; Axon Instruments, Foster City, CA), which was also used to control the D/A converter for generation of voltage clamp protocols and analysis of generated data. Some of the data fitting was done using Sigma Plot for windows (V.1.02; Jandel Scientific, CA) and final figure preparation was done with Corel DRAW (V.3.0; Corel Corp., Salinas, CA).

Step voltage pulses, from a holding potential of 0 mV, increasing and decreasing in steps of 10 mV, or voltage ramps with 5 mV steps of 400 msec duration, in both hyperpolarized and depolarized directions were applied to the patches. cAMP-activated currents were obtained from the difference between recordings in control solutions (with no cAMP) and solutions with added cAMP or 8-Bromo-cAMP. Both voltage steps and ramps yielded similar results. All voltages are expressed with the standard sign convention (i.e., the potential of internal with respect to the external membrane surfaces). Liquid junction potentials were calculated for the solutions with added divalent ions (ranging from 0.7 to 1.6 mV) using the software program *JPCalc* (Barry, 1994) and appropriate corrections applied to the membrane potential. The current traces shown in all figures are examples of current responses at +60 and at −60 mV, obtained after background subtraction. To construct dose-response curves, the average steady-state currents measured at −60 mV were normalized with respect to the current activated by 1,000 μM cAMP (I_{norm}) in the control (0 Ca) solution, in the same patch. The data points were averaged from 4 to 11 patches and the error bars represent ±SEM.

Results

The primary aim of this paper was to determine whether intracellular Ca^{2+} reduces the cAMP affinity of the olfactory CNG channel by a novel endogenous factor in

addition to calmodulin. The previous observation that the Ca^{2+}-induced reduction in the affinity of the channel for cAMP is lost irreversibly by exposure of the patch to 3 mM Mg^{2+} + 2 mM EGTA (Mg + EGTA; Lynch & Lindemann, 1994) has been used to endeavor to achieve this aim. It was also hoped that these experiments would help to elucidate the mechanism underlying this Mg + EGTA effect.

Membrane patches excised from the dendritic knobs of the ORNs in an inside-out configuration were exposed to 1, 10, 100 and 1,000 μM cAMP applied to the cytosolic side in 0 Ca (control) solutions and voltage steps were applied (*see* Materials and Methods) to elicit macroscopic currents. The saturating current at −60 mV in 1,000 μM cAMP, in the absence of divalent cations, ranged from 112–1024 pA. Also, the magnitude of the saturating current at +60 mV with 1000 μM cAMP was not very different from its magnitude at −60 mV in each experiment. Figure 1*C* shows an example of the current traces recorded at +60 and −60 mV, when 1, 10 or 1000 μM cAMP were added to control (0 Ca) solutions, with background leakage currents subtracted. The current elicited by 10 μM cAMP is clearly almost saturating under these conditions.

As demonstrated previously, micromolar concentrations of Ca^{2+} are ineffective in inhibiting the cAMP-activated current in the rat olfactory CNG channels, both in cloned and native channels (Chen & Yau, 1994; Lynch & Lindemann, 1994). Hence, a concentration of 0.2 mM Ca^{2+} was chosen to obtain a clearly demonstrable reduction of cAMP affinity.

Examples of current traces recorded at +60 and −60 mV, when 1, 10 or 1,000 μM cAMP were applied in the presence of 0.2 Ca, (through the same patch of membrane as in Fig. 1*C*) are shown in Fig. 1*D*. Averaged results from six experiments at −60 mV, plotted as dose-response relationships, are shown in Fig. 1*E*. The data were fitted by a curve using a Hill-type equation:

$$I_{\text{norm}} = C^h/[C^h + \text{EC}_{50}{}^h] \quad (1)$$

where I_{norm} is the normalized current, C is the cyclic nucleotide concentration and h is the Hill coefficient. In the absence of divalent ions the EC_{50} was 3.2 μM cAMP and the Hill coefficient (h) was 1.6. Curves generated using these parameters have also been used to fit 0 Ca solution data in Figs. 3 and 4. However, although 0.2 Ca had little effect on the Hill coefficient (h = 1.2) it did cause the EC_{50} to be increased by a factor of approximately 10-fold (*see* Table).

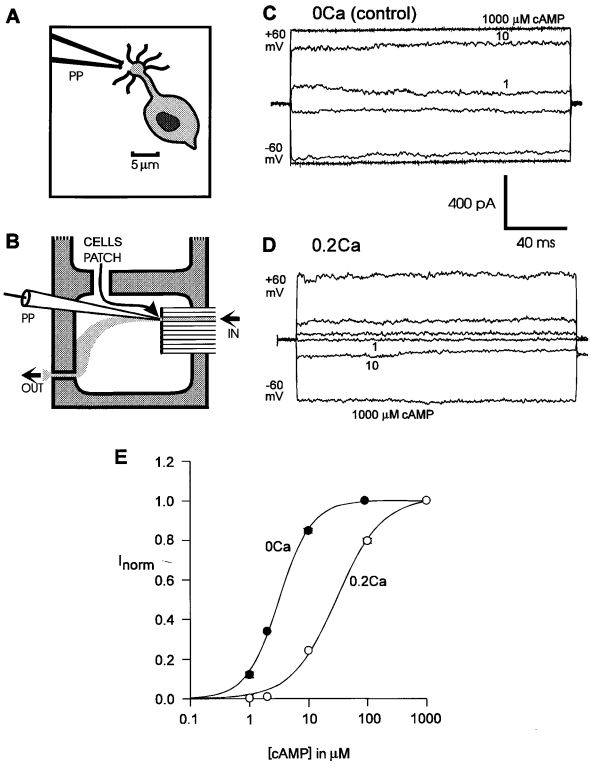

Fig. 1. Ca^{2+}-dependent inhibition of cAMP-gated currents in membrane patches from dendritic knobs of olfactory receptor neurons (ORNs). (*A*): membrane patches were obtained from the dendritic knob amidst the cilia of an ORN. (*B*): diagram of the perfusion system. Cells were plated in a separate compartment and the patch pipette (PP) with an inside-out membrane patch was moved to another compartment through a narrow channel and positioned in front of one of a group of tubes through which different test solutions flowed. (*C*) and (*D*): Examples of CNG currents recorded at +60 and −60 mV in 0 Ca solution (control) and in 0.2 Ca (with 0.2 mM Ca^{2+}), in the presence of 1, 10 and 1000 μM cAMP, as indicated. Voltage pulses were applied in steps of 10 mV from −80 to +70 mV from a holding potential of 0 mV, for a duration of 180 msec. The respective background traces in the absence of cAMP have been subtracted. Scale bars apply to both sets of traces. (*E*): cAMP dose-response relationships in control (0 Ca) solution and in 0.2 Ca solution. Data points are averaged values of current at −60 mV from six patches, normalized (I_{norm}) to the maximum current obtained in the presence of 1,000 μM cAMP in the control (0 Ca) solution for the respective patch. In this and all subsequent figures, error bars represent the SEM and are shown when larger than symbol size. Curves were fitted by a Hill type equation, using an EC_{50} of 3.2 μM cAMP (Hill-coefficient, h = 1.6) for 0 Ca and an EC_{50} of 30.2 μM cAMP (h = 1.2) for 0.2 Ca.

Decrease in the cAMP Sensitivity by Ca^{2+} Does Not Wash Out with Time

Examples of current traces in the 0 Ca (control) solution and in 0.2 Ca (with added 0.2 mM Ca^{2+}) are shown at 5 and 15 min after patch excision in Fig. 2*A*, with 10 and 100 μM cAMP. This clearly illustrates that the inhibitory effect of Ca^{2+} on the CNG currents activated by cAMP does not wash out with time and is readily reversible. The ratio of currents, measured at 10 μM cAMP with respect to 100 μM cAMP (I_{10}/I_{100}) in the presence of 0.2 Ca solution, from four different patches is plotted against time in Fig. 2*C*. This ratio remained constant at 0.25 ± 0.02 for at least 15 min.

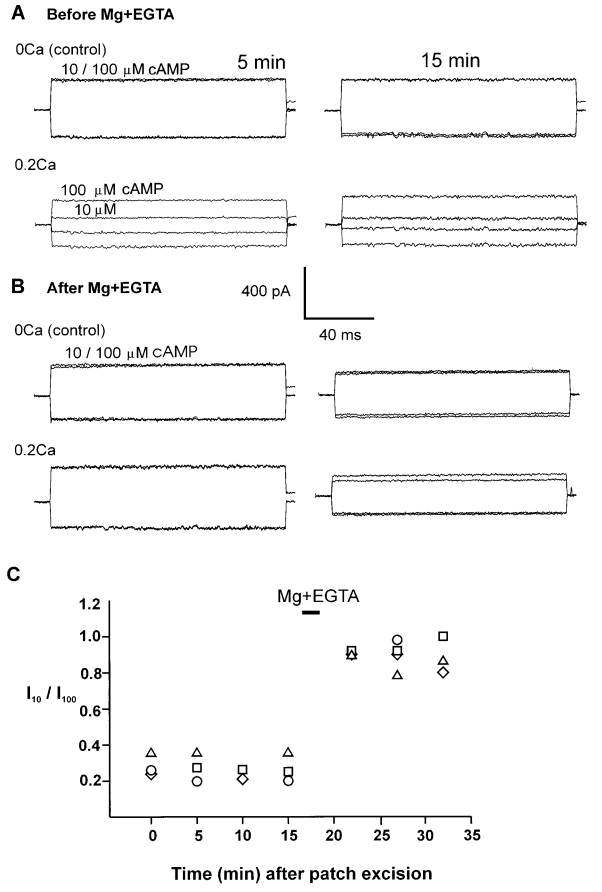

Fig. 2. Ca^{2+}-induced inhibition of CNG currents does not wash out with time. However, subsequent exposure of patches to a Mg + EGTA solution (containing 3 mM Mg^{2+} + 2 mM EGTA) removes the ability of Ca^{2+} to induce inhibition. (*A*): CNG currents recorded at +60 mV (top traces in each panel) and −60 mV (bottom traces, in each panel) in 0 Ca (control) solution and in 0.2 Ca solution (with 0.2 mM Ca^{2+}) when 10 and 100 μM cAMP were added, at 5 min (left panel) and 15 min (right panel) after patch formation before exposure to Mg + EGTA. All current recordings were from the same patch. (*B*): CNG current responses at −60 and +60 mV for the same patch as in (*A*) after exposure to Mg + EGTA for 2 min, with the left panel showing the response after 5 min, and the right panels after 15 min. The time-dependent decrease in the maximum current amplitude, displayed here, was not usually observed in other patches. The scale bar applies to all traces. (*C*): The ratio of the currents obtained with 10 μM cAMP to that with 100 μM cAMP for 0.2 Ca (I_{10}/I_{100}) are plotted as a function of time for four different patches. The ratio (I_{10}/I_{100}) of 0.25 ± 0.02 for the native patch before Mg + EGTA exposure was increased to 0.89 ± 0.02 after Mg + EGTA exposure.

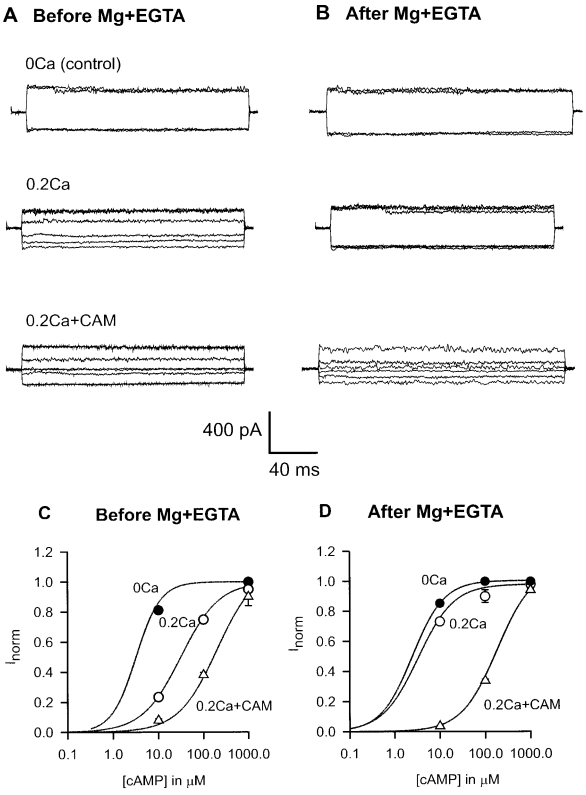

Fig. 3. Effect of 0.2 mM Ca^{2+} and exogenously applied CAM on the CNG currents before and after exposure to a Mg + EGTA solution (containing 3 mM Mg^{2+} + 2 mM EGTA). (*A*) and (*B*): All data were from the same patch. All panels show currents activated at +60 and −60 mV when 10, 100 and 1000 μM cAMP were applied. The top panels give the responses in 0 Ca (control) solution (only responses to 10 and 1,000 μM cAMP are shown), the center panels the responses in 0.2 Ca solution and the lowest panels the responses in 0.2 Ca + CAM solution. The scale bars apply to all traces. (*C*) and (*D*): cAMP dose-response relationships in 0 Ca, 0.2 Ca and 0.2 Ca + CAM, before and after exposure to Mg + EGTA. Results were averaged from eleven patches, normalizing the current value at −60 mV to the value with 1,000 μM cAMP, as described for Fig. 1. Curves were fitted by a Hill type equation (*see* the Table for parameters), with the 0 Ca curve being generated from the Hill parameters for the 0 Ca curve in Fig. 1.

Irreversible Loss of Affinity Shift Caused by the Exposure of the Patch to 3 mM Mg^{2+} + 2 mM EGTA

The cAMP affinity shift caused by 0.2 Ca solution was lost irreversibly on exposure of the patch to 3 mM Mg^{2+} + 2 mM EGTA (Mg + EGTA) for 2 min as previously found by Lynch and Lindemann (1994). The ratio, I_{10}/I_{100}, in 0.2 Ca after Mg + EGTA exposure, increased to 0.89 ± 0.02 as shown in Fig. 2*C*. Examples of CNG currents activated by cAMP in 0 Ca (control) solution and in 0.2 Ca, 5 and 15 min after the same patch was exposed to 3 mM Mg^{2+} for a period of 2 min (Fig. 2*B*), clearly show that the inhibitory effect of 0.2 Ca is lost irreversibly. It should also be noted that in most of the patches the magnitude of the current in 0 Ca solution did not change significantly throughout the experiment, although there was a small change observed occasionally, as in the specially timed examples given in Fig. 2*B*.

Exogenous Calmodulin (CAM) Decreases the Affinity of the CNG Channel for cAMP

The effect of applying 0.2 mM Ca^{2+} together with 470 nM CAM (0.2 Ca + CAM) to the intracellular side of the

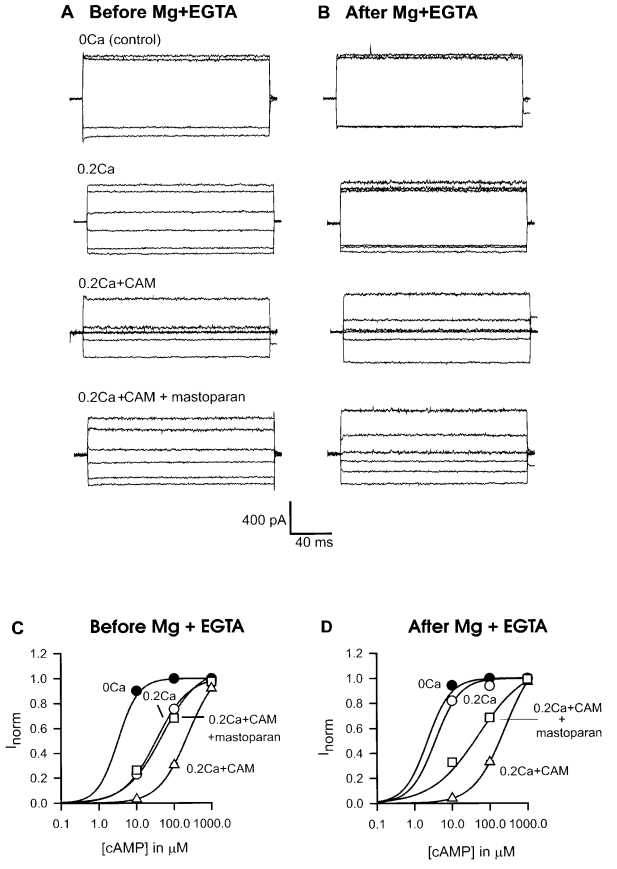

Fig. 4. The effect of Ca^{2+}, CAM and mastoparan on the CNG currents, before and after exposure to a Mg + EGTA solution. (*A*) and (*B*): CNG current traces recorded at +60 and −60 mV in 0 Ca solution, in 0.2 Ca, in 0.2 Ca + CAM and in 0.2 Ca + CAM + mastoparan when 10, 100 and 1,000 μM cAMP were added to the test solutions before and after Mg + EGTA exposure. CNG current inhibition by 0.2 Ca + CAM is reversed by the addition of mastoparan. All sets of current traces were recorded from the same patch and the scale bars apply to all traces. (*C*) and (*D*): cAMP dose-response relationships with averaged normalized currents from eight patches at −60 mV in the different test solutions, before and after Mg + EGTA exposure. Curves were fitted using a Hill type equation (*see* the Table for parameters), with the 0 Ca curve being generated from the Hill parameters for the 0 Ca curve in Fig. 1.

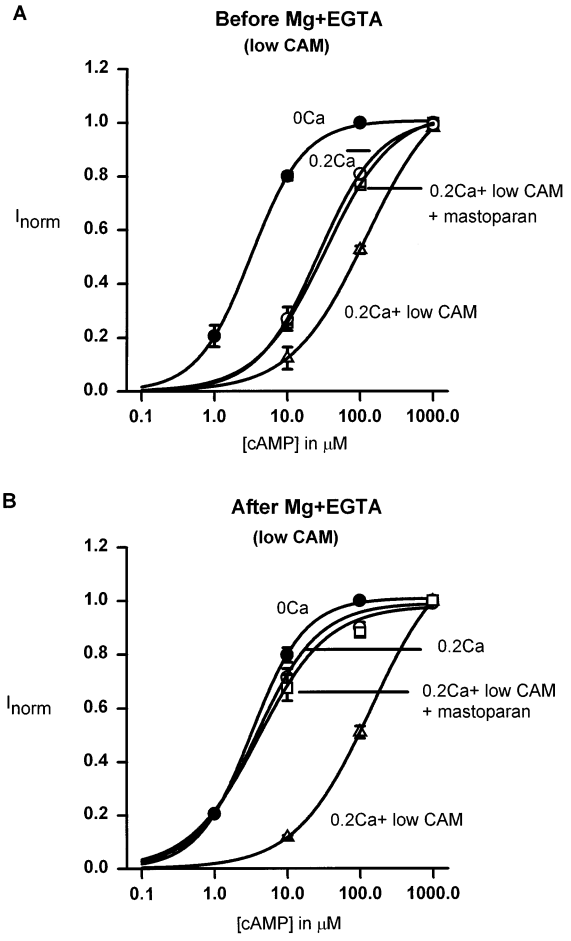

Fig. 5. The efficacy of mastoparan antagonism of the calmodulin-mediated affinity shift is increased following Mg + EGTA exposure. A low calmodulin concentration of 120 nM was used in these experiments. (*A*) and (*B*) cAMP dose-response relationships with averaged normalized currents from 3–5 patches at −60 mV in 0 Ca solution, in 0.2 Ca solution, in 0.2 Ca + low CAM solution and in 0.2 Ca + low CAM + mastoparan solution, before and after Mg + EGTA exposure. Averaged curve fit parameters are given in the Table.

excised dendritic knob membrane patches was also studied. Under conditions of both 0.2 Ca and 0.2 Ca + CAM, currents were measured at 10, 100 and 1000 μM cAMP. As seen in the example in Fig. 3*A*, 0.2 Ca + CAM caused a much greater affinity shift than did 0.2 Ca. Furthermore, following a 2-min exposure to Mg + EGTA, the affinity shift induced by 0.2 Ca is abolished (Fig. 3*B*), but the affinity shift caused by 0.2 Ca + CAM is not affected. Averaged normalized current responses from eleven patches at −60 mV, plotted as cAMP dose-response relationships, before and after Mg + EGTA exposure, are shown in Fig. 3*C* and *D*, for the 0 Ca, 0.2 Ca and 0.2 Ca + CAM solutions. The curve through the data points was generated using the previously measured EC_{50} and *h* values for the 0 Ca solution. Both the 0.2 Ca effect and the 0.2 Ca + CAM effect were fully and rapidly reversible. As shown in Fig. 3*D*, there is clearly a loss of affinity shift induced by 0.2 Ca after Mg + EGTA exposure, whereas the 0.2 Ca + CAM induced cAMP affinity shift is unaffected. Parameters of curve fits before and after Mg + EGTA exposure, for this and all subsequent experiments are given in the Table.

Effect of Mastoparan on Ca^{2+} + CAM and Ca^{2+}-only Affinity Shifts

To determine whether the Ca^{2+} + CAM and the Ca^{2+}-only effect are mediated by different mechanisms, the effect of CAM antagonist, mastoparan, was examined. Mastoparan was used at a concentration of 10 μM, unless otherwise noted, since it was shown that this concentra-

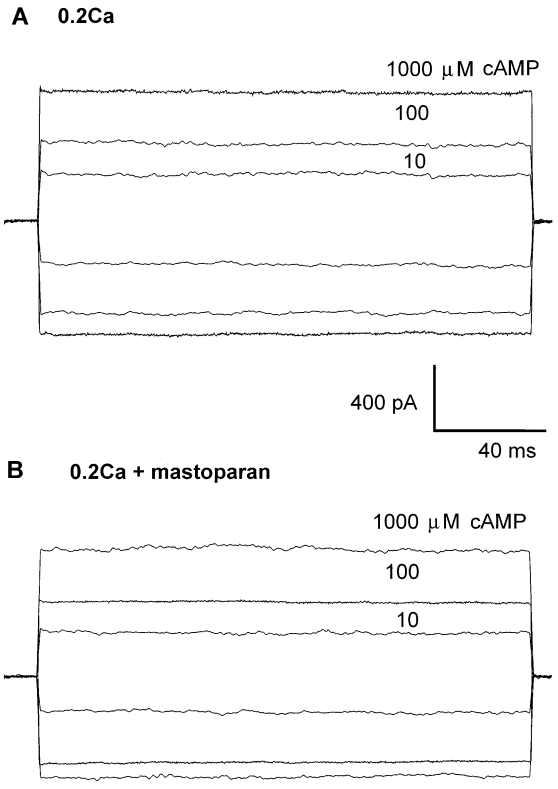

Fig. 6. Mastoparan had no effect on Ca^{2+}-mediated inhibition in the absence of exogenous calmodulin. (*A*) Current responses at +60 and −60 mV, when 10, 100 and 1,000 μM cAMP were added to 0.2 Ca solutions (*B*) Similar experimental protocol in the same patch but in the presence of 0.2 Ca + mastoparan solutions (0.2 Ca + 10 μM mastoparan; *B*).

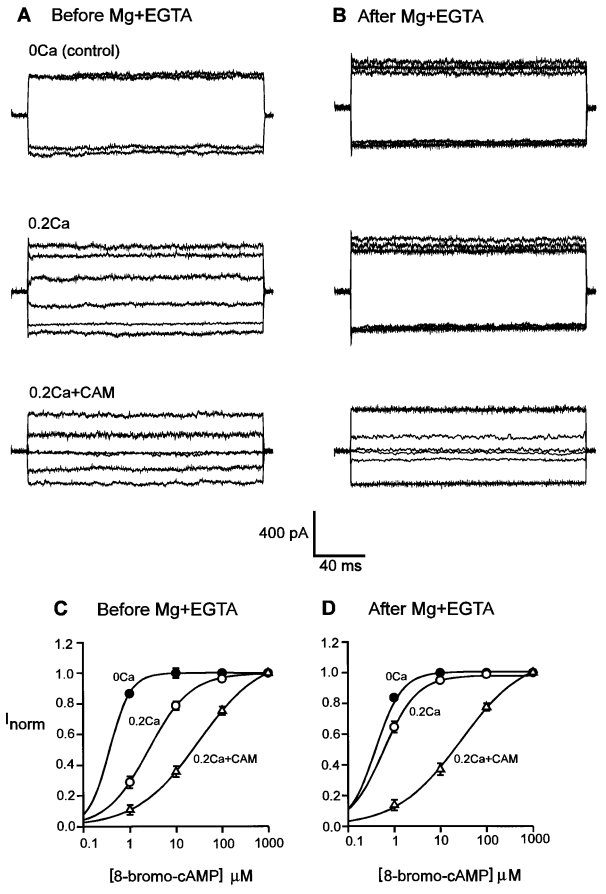

Fig. 7. Effect of Ca^{2+} and exogenously applied calmodulin on CNG currents activated by 8-bromo-cAMP, a phophodiesterase resistant analogue of cAMP. (*A*) and (*B*): Currents elicited at +60 and −60 mV in 0 Ca solution, in 0.2 Ca and 0.2 Ca + CAM in the presence of 1, 10 and 100 μM 8-bromo-cAMP, before and after exposure of the patch to a Mg + EGTA solution. The current recordings are all from the same patch and the scale bars apply to all traces. CNG channels are more sensitive to this analogue of cAMP. However, the responses to added Ca^{2+} and CAM are similar to those obtained with cAMP, except that the effective concentrations were 10-fold smaller. (*C*) and (*D*): The dose-response relationships for 8-bromo-cAMP, before and after exposure of the patches to Mg + EGTA. Results were averaged from five patches at −60 mV, normalized to the value of 100 μM 8-bromo-cAMP in control solutions. Continuous lines to the data points were fitted using a Hill-type equation (*see* the Table for parameters).

tion does not induce nonspecific inhibition of these channels (Kleene, 1994).

Following control measurements in 0 Ca solution, the membrane patches were exposed to 0.2 Ca solution and then to 0.2 Ca + CAM, both in the absence and in the presence of mastoparan (0.2 Ca + CAM + mastoparan). This protocol was repeated after Mg + EGTA exposure. Figure 4*A* shows examples of current responses at −60 and +60 mV in the respective experimental solutions before Mg + EGTA exposure and Fig. 4*B* shows recordings from the same patch after exposure to Mg + EGTA for 2 min. It is clear from Fig. 4*A* and *B* (0.2 Ca + CAM and 0.2 Ca + CAM + mastoparan), that the current inhibition caused by calmodulin is antagonized by mastoparan.

These current responses in 0 Ca (control) and 0.2 Ca solutions, before and after Mg + EGTA (Fig. 4*A* and *B*), were as expected, very similar to the previous experiments (e.g., Figs. 2 and 3). The averaged cAMP dose-responses before and after Mg + EGTA from eight patches are shown in Fig. 4*C* and *D* and all the curve fit parameters are given in the Table.

Although the reversal of the CAM effect by mastoparan was complete before Mg + EGTA (Fig. 4*C*), it was not complete after Mg + EGTA exposure of the patch (Fig. 4*D*). Since the concentration of mastoparan used was more than about twenty times that of CAM, lack of availability of the antagonist was not likely to be the reason for the incomplete reversal of the CAM effect after Mg + EGTA exposure. The mechanism underlying the decreased effectiveness of mastoparan after Mg + EGTA exposure was therefore investigated. Higher concentrations of mastoparan caused a block of the CNG current at all concentrations of cAMP (*data not shown*).

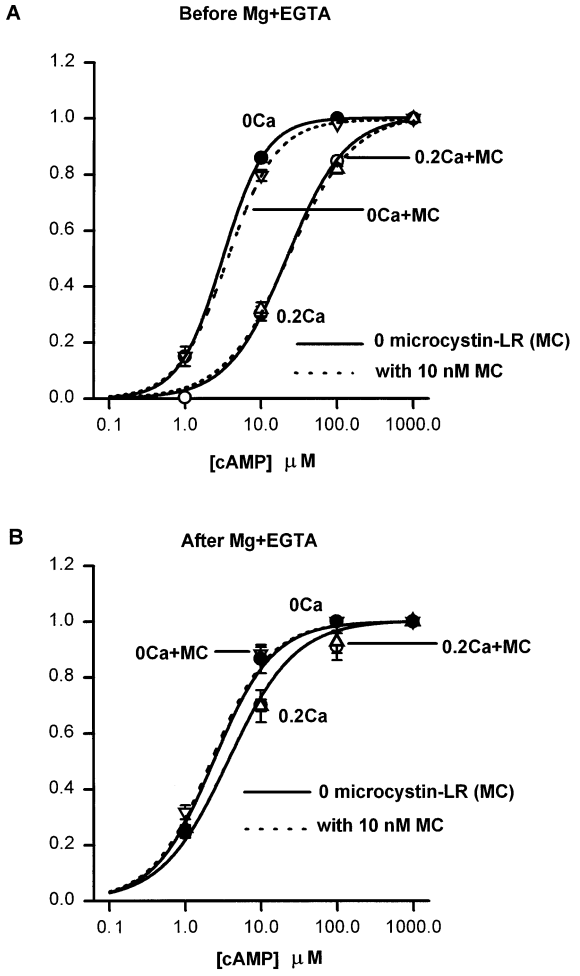

Fig. 8. Addition of the protein phosphatase inhibitor, microcystin-LR (MC) had no significant effect on the cAMP dose-response relationships in 0 Ca and 0.2 Ca solutions before and after Mg + EGTA exposure. (*A*) and (*B*) cAMP dose-response relationships with averaged normalized currents from 4 patches at −60 mV in the presence (0 Ca + MC; 0.2 Ca + MC) and in the absence of added 10 nM microcystin (0 Ca; 0.2 Ca). Averaged curve fit parameters are given in the Table.

Hence a lower concentration of CAM (120 nM) was used together with 10 μM mastoparan. As seen in Fig. 5*A* and *B*, which shows the cAMP dose-response curves with 120 nM CAM + 0.2 mM Ca^{2+} (0.2 Ca + low CAM), with and without 10 μM mastoparan, there is now a complete reversal of the effect of CAM by mastoparan following Mg + EGTA exposure. This would seem to indicate that the sensitivity of the channel for CAM is increased following the loss of an endogenous factor that is removed by Mg + EGTA exposure.

It was necessary to determine whether mastoparan was able to antagonize the Ca^{2+}-only effect, to test the possibility that *endogenous* calmodulin may have resulted in the reduced affinity of the channel for cAMP. This possibility was eliminated as there was no change in the current responses obtained with 0.2 Ca + mastoparan when compared with 0.2 Ca alone before Mg + EGTA (Fig. 6*A* and *B*).

Ca^{2+}-only and Ca^{2+} + CAM Effects are still Present with Hydrolysis-resistant Analogue 8-Bromo-cAMP

The effect of Ca^{2+} + CAM involves direct interaction with the CNG channel (Liu et al., 1994). Ca^{2+}-calmodulin-activated phosphodieterase (PDE) has been found predominantly in the olfactory cilia (Borisy et al., 1992) and it was considered that this might reduce the effective concentration of cAMP around the channel. To determine whether or not the Ca^{2+} + CAM effect on the CNG channel in our study is mediated by the olfactory PDE, experiments were repeated using 8-bromo-cAMP, which is resistant to hydrolysis by PDE. When 8-bromo-cAMP was used to activate the CNG channels, it was found that the channels were more sensitive to this analogue of cAMP and that the EC_{50} was now 370 nM in the absence of added divalent cations. Because of this, the concentrations of 8-bromo-cAMP used in the control solution were 1 and 100 μM for the 0 Ca (control) solution and 1, 10 and 100 μM for the 0.2 Ca and 0.2 Ca + CAM solutions. Examples of the current traces at +60 and −60 mV are shown in the different experimental solutions, before and after Mg + EGTA exposure in Fig. 7*A* and *B*.The data averaged from five patches at −60 mV in each case normalized to the value obtained in the presence of 100 μM 8-bromo-cAMP for the corresponding patch are shown in Fig. 7*C* and *D*. Thus 8-bromo-cAMP has no different effect on either the Ca^{2+}-only effect or the Ca^{2+} + CAM effect, ruling out the involvement of phophodiesterases in mediating either effect. The values of the Hill coefficients (*h*) along with the EC_{50} values used to fit the data points are given in the Table.

Ca^{2+}-only Effect is Present in the Presence of the Phosphatase Inhibitor, Microcystin-LR

We also considered the possibility of a Ca^{2+}-only effect mediated by the inhibition of an endogenous phosphatase associated with the CNG channel, as was previously reported for the cGMP-activated photoreceptor channel (Gordon et al., 1992). We compared the cAMP affinity shift induced by 0.2 Ca solution with (0.2 Ca + MC) and without 10 nM microcystin-LR, a protein phosphatase inhibitor, before and after Mg + EGTA exposure of the patches of membranes (Fig. 8*A* and *B*). As seen in Fig. 8*A*, the cAMP affinity shift induced by 0.2 Ca is maintained in the presence of microcystin-LR prior to Mg + EGTA exposure. This clearly indicates that phosphatase is not involved in mediating the Ca^{2+}-only effect since we would expect to see a loss of the Ca^{2+}-induced affin-

Table. EC_{50}s and Hill coefficients (*h*) calculated using the average results of normalized currents at −60 mV, through the CNG channels in dendritic knob patches from olfactory neurons.

Experiment	Solutions	Before Mg+EGTA exposure		After Mg+EGTA exposure	
		EC_{50} (μM)	*h*	EC_{50}(μM)	*h*
Ca^{2+}/CAM/cAMP	0.2 Ca	31.3	1.15	3.3	1.1
(Fig. 3)	0.2 Ca + CAM	201	1.0	203	1.1
Ca^{2+}/CAM/mastoparan cAMP	0.2 Ca	33.4	1.1	3.6	1.3
(Fig. 4)	0.2 Ca + CAM	235	1.12	255	1.04
	0.2 Ca + CAM + mastoparan	47.4	0.91	51.2	0.7
Ca^{2+}/CAM/ 8-Bromo-cAMP	0 Ca	0.37	1.9	0.39	1.5
(Fig. 7)	0.2 Ca	2.6	1.0	0.59	1.1
	0.2 Ca + CAM	31.1	0.65	28.1	0.63

EC_{50}s and Hill coefficients (h) were recorded in various test solutions and used to fit the data points in the graphs showing cAMP dose-response relationships (Figs. 3, 4, and 7). Details of the solutions are given in Materials and Methods.

ity shift on addition of microcystin-LR if an endogenous phosphatase was involved. As expected, addition of microcystin-LR to 0.2 Ca after Mg + EGTA exposure (Fig. 8*B*) similarly did not affect the loss of affinity shift for cAMP.

Discussion

In this report, we confirm the previous finding that Ca^{2+} application alone causes about a 10-fold decrease in cAMP affinity for the olfactory CNG channel (Lynch & Lindemann, 1994) and we show that the same concentration of Ca^{2+} in the presence of 470 nM calmodulin induces a further 10-fold decrease in the cAMP affinity. The Ca^{2+} + CAM-mediated affinity reduction is selectively antagonized by mastoparan, whereas the Ca^{2+}-only effect is selectively abolished by a 2 min exposure to a solution containing 3 mM Mg^{2+} + 2 mM EGTA.

In principle, the Ca^{2+}-only effect could have been caused by either endogenous CAM or by an unknown regulatory factor. However, the latter option is more likely because: (i) patch exposure to control solution with EGTA and no Mg^{2+} in the solution does not cause a wash out of the effect (Lynch & Lindemann, 1994), whereas it does do so when CAM is tightly bound to CNG receptor-channels in other preparations (e.g., Chen et al., 1994; Saimi & Ling, 1995); (ii) reapplication of calmodulin, after ablation of the Ca^{2+}-only effect by Mg + EGTA, does not restore the effect; (iii) the Ca^{2+}-only effect is insensitive to mastoparan. This third point should be interpreted cautiously, since mastoparan binds directly to calmodulin and may not be able to do so if calmodulin is tightly bound to the receptor-channel complex (and possibly also to the membrane). Hence, it is most likely that in intact cells Ca^{2+} affects channel affinity by both a calmodulin-sensitive mechanism and a second distinct mechanism that is mediated by a tightly bound regulatory factor. There is no evidence for a direct Ca^{2+} inhibitory site on the channel as proposed by Zufall, Shepherd and Firestein (1991).

Although mastoparan completely antagonizes the Ca^{2+} + CAM effect prior to Mg + EGTA exposure, an unexpected observation was that it only partially antagonizes the Ca^{2+} + CAM effect after Mg + EGTA exposure (Fig. 4*C* and *D*). Addition of a lower concentration of CAM (120 nM) along with the same concentration of (10 μM) mastoparan caused a complete reversal of the CAM effect after Mg + EGTA exposure (Fig. 5*A* and *B*) suggesting that removal of the unknown regulatory factor by Mg + EGTA causes an increase in the CAM affinity for its binding site.

The presence of the Ca^{2+}-only and the Ca^{2+} + CAM-effect in the presence of the nonhydrolyzable analogue, 8-bromo cAMP rules out the role of phosphodiesterases in mediating the effect. Similarly, there was no change in the affinity shift induced by 0.2 Ca when microcystin-LR was added to block the endogenous phosphatase, ruling out the possibility of phosphorylation of the channel playing a part in the Ca-only effect.

Mg^{2+} does not activate CAM in the photoreceptor system (Hsu & Molday, 1993). It is also known that in the presence of Mg^{2+}, CAM is prevented from forming an active complex with Ca^{2+}, and that it is inactive in a Mg^{2+}-bound form in eukaryotic cells (Okhi et al., 1993). In principle, the two possible ways in which Mg + EGTA could be removing the Ca^{2+}-induced cAMP affinity for the CNG channel would seem by (i) inactivating CAM or (ii) washing away a factor associated with the receptor-

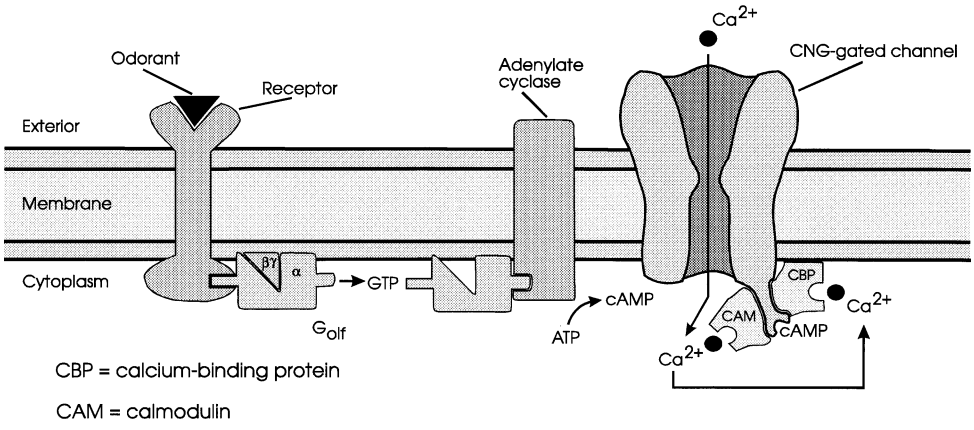

Fig. 9. A schematic diagram of a section of olfactory receptor membrane illustrating a model for the activation and inhibition of CNG channels. It is proposed that these channels have two sites of action for intracellular Ca^{2+}. One is Ca^{2+}-CAM site and the other is occupied by an unknown endogenous calcium binding-protein (CBP). In both cases, Ca^{2+} binding reduces the sensitivity for cAMP. In excised patches, CAM is washed out and must be added exogenously, whereas CBP remains tightly associated with the channel but is ablated by Mg + EGTA exposure. This is an extension and modification of the model of Kramer and Siegelbaum (1992); *see* their Fig. 9).

channel complex. From the results of our study it is clear that the second option must be involved, as there is loss of an additional factor by Mg + EGTA exposure distinct from CAM since exogenous application of CAM did not restore the calcium induced affinity shift. From our experiments we cannot also rule out the inactivation of CAM by Mg^{2+} in vivo.

Figure 9 shows a schematic diagram of a section of membrane with a model of the mechanisms contributing to the activation and inactivation of the olfactory CNG channel. This suggests the role of Ca^{2+} in acting on the CNG channel, through the mediation of CAM, as well as through the mediation of a possible endogenous calcium binding protein (CBP) to alter the sensitivity of the channel for the binding of cAMP. The action of Ca^{2+} ions at both sites could contribute to a rapid and effective negative feedback loop, which could account for the short term adaptation of the response to sustained odour exposure as seen in intact neurons (Kurahashi & Shibuya, 1990).

Comparison with Other Studies

The dramatic reduction in the affinity of the CNG channels for cAMP upon addition of Ca^{2+} + CAM confirms the recent reports describing the direct action of Ca^{2+} + CAM on a binding site in the olfactory CNG channel, both in cloned as well as in native channels (Chen & Yau, 1994; Liu et al., 1994). Our study differs from the study of the effect of intracellular Ca^{2+} on the CNG channels in the catfish ORNs (Kramer & Siegelbaum, 1992) in several respects: (i) we did not find any measurable inhibitory effect at micromolar concentrations of Ca^{2+} (ii) the inhibition induced did not wash out with time and (iii) there is evidence for intracellular Ca^{2+} acting via CAM as well as through a distinct regulatory factor which is not a PDE or phosphatase.

Inhibition of single olfactory CNG channels from the salamander by low micromolar Ca^{2+} concentrations was observed at a saturating cAMP concentration (Zufall et al., 1991). Such a potent inhibitory effect is inconsistent with the results of either Kramer and Siegelbaum (1992), Chen and Yau (1994) or the present study, suggesting that the salamander CNG channel may express a novel calcium-dependent inhibitory mechanism. The possibility of species-dependent peculiarities of the salamander olfactory CNG channel is also suggested by the unusually high single channel conductance (40 pS) and the low density of CNG channels in the dendritic knob (Zufall et al., 1991).

Not surprisingly, there are striking similarities between the modulatory mechanisms of the olfactory and photoreceptor CNG channels. In the photoreceptor CNG channel, which is directly activated by cyclic 3′,5′-guanosine monophosphate (cGMP) and has extensive amino acid sequence identity with its olfactory counterpart, Ca^{2+} reduces the apparent affinity of the channel for cGMP via a calmodulin-dependent mechanism (Kaupp & Koch, 1992; Hsu & Molday, 1993; Nakatani et al., 1995). A recent report on the photoreceptor CNG channel has also suggested that in excised patches Ca^{2+} acts through calmodulin as well as through another mechanism involving a distinct endogenous factor (Gordon et al., 1995).

Ca^{2+} may act at several sites in olfactory neurons to effect a role in the termination of the odor response. Borisy et al. (1992) showed that Ca^{2+}-dependent and -independent mechanisms activate PDE which hydrolyzes cAMP thereby reducing the apparent cAMP sensi-

tivity of the olfactory CNG channels. An increase in intracellular Ca^{2+} can occur by influx through the CNG channels (Kurahashi & Shibuya, 1990; Frings et al., 1995) to initiate the termination of the signal. However, the finding that Ca^{2+} can also increase the cAMP concentration by increasing the activity of the adenylyl cyclase through activation of calmodulin (Frings, 1993), may also need to be considered in any explanation of the overall response of these CNG channels to odorant activation.

Physiological Role

The mechanism of channel modulation by divalent cations is particularly relevant physiologically, because an increase in intracellular Ca^{2+} concentration occurs upon odorant stimulation. The olfactory cilia are embedded in mucus containing about 0.3 mM Ca^{2+} (Chiu, Nakamura & Gold, 1989). At millimolar concentrations of external Ca^{2+} these channels carry a pure Ca^{2+} current (Frings et al., 1995). Hence, like voltage-gated Ca^{2+} currents, it is quite possible that the free Ca^{2+} could reach hundreds of micromolar within the ciliary and dendritic knob regions following odorant stimulation (Smith & Augustine, 1988; Augustine & Neher, 1992; Llinàs, Sugimori & Silver 1992; Fryer & Zucker, 1993; Jaworsky et al., 1995). The rise in Ca^{2+} could then regulate its own entry through the CNG channels by decreasing the sensitivity of the channels for cAMP through the action of a calcium binding protein (CBP) as well as through activation of calmodulin. The decrease in the sensitivity of the CNG channel for cAMP brought about by Ca^{2+} by multiple mechanisms could provide a fast and effective short-term adaptation of an olfactory response.

This work was supported by the Australian Research Council of Australia.

References

Augustine, G.J., Neher, E. 1992. Calcium requirements for secretion in bovine chromaffin cells. *J Physiol.* **450:**247–271

Balasubramanian, S., Lynch, J.W., Barry, P.H. 1995*a*. Role of internal Ca^{2+}, Mg^{2+} and calmodulin in the agonist affinity of mammalian olfactory cAMP-gated channels. *Proc. Aust. Physiol. Pharmacol. Soc.* **26:**152*P*

Balasubramanian, S., Lynch, J.W., Barry, P.H. 1995*b*. The permeation of organic cations through cAMP-gated channels in mammalian olfactory receptor neurons. *J. Membrane Biol.* **146:**177–191

Barry, P.H. 1994. JPCalc, a software package for calculating liquid junction potential corrections in patch-clamp, intracellular, epithelial and bilayer measurements and for correcting junction potential measurements. *J. Neurosci. Methods* **51:**107–116

Boekhoff, I., Tareilus, E., Strotmann, J., Breer, H. 1990. Rapid activation of alternate second messenger pathways in olfactory cilia from rats by different odorants. *EMBO J.* **9:**2453–2458

Borisy, F.F., Ronnett, G.V., Cunningham, A.M., Juilfs, D., Beavo, J., Snyder, S.H. 1992. Calcium/calmodulin-activated phosphodiesterase expressed in olfactory receptor neurons. *J. Neurosci.* **12:**915–923

Chen, T.Y., Idling, M., Molday, L.L., Hsu, Y.T., Yau, K.W., Molday, R.S. 1994. Subunit 2 (or β) of retinal rod cGMP-gated cation channel is a component of the 240-kDa channel-associated protein and mediates Ca^{2+}-calmodulin modulation. *Proc. Natl Acad. Sci. USA* **91:**11757–11761

Chen, T.Y., Yau, K.W. 1994. Direct modulation by Ca^{2+}-calmodulin of cyclic nucleotide-activated channel rat olfactory receptor neurons. *Nature* **368:**545–548

Chiu D., Nakamura, T., Gold, G.H. 1989. Ionic composition of toad olfactory mucus measured with ion selective microelectrodes. *Chem. Senses* **13:**677–678

Frings, S. 1993. Protein kinase C sensitizes olfactory adenylate cyclase. *J. Gen. Physiol.* **101:**183–205

Frings, S., Seifert, R., Godde, M., Kaupp, U.B. 1995. Profoundly different calcium permeation and blockage determine the specific function of distinct cyclic nucleotide-gated channels. *Neuron* **15:**169–179

Fryer, M.W., Zucker, R.S. 1993. Ca^{2+}-dependent inactivation of Ca^{2+} current in Aplysia neurons: kinetic studies using photolabile Ca^{2+} chelators. *J. Physiol.* **464:**501–528

Gordon, S.E., Brautigan, D.L., Zimmerman, A.L. 1992. Protein phosphatases modulate the apparent agonist affinity of the light-regulated ion channel in the retinal rods. *Neuron* **9:**739–748

Gordon, S.E., Downing-Park, J., Zimmerman, A.L. 1995. Modulation of the cGMP-gated ion channel in frog rods by calmodulin and an endogenous inhibitory factor. *J. Physiol.* **486:**533–546

Hamill, O.P., Marty, A., Neher, E., Sakmann, B., Sigworth, F.J. 1981. Improved patch-clamp techniques for high-resolution current recording from cells and cell-free membrane patches. *Pfluegers Arch.* **391:**85–100

Hsu, Y.E., Molday, R.S. 1993. Modulation of the cGMP-gated channel of rod photoreceptor cells by calmodulin. *Nature* **361:**76–79

Jaworsky, D.E., Matsuzaki, O., Borisy, F.F., Ronnett, G.V. 1995. Calcium modulates the rapid kinetics of the odorant-induced cyclic AMP signal in rat olfactory cilia. *J. Neurosci.* **15:**310–318

Kaupp, U.B., Koch, K.W. 1992. Role of cGMP and Ca^{2+} in vertebrate photoreceptor excitation and adaptation. *Ann. Rev. Physiol.* **54:**153–175

Kleene, S.J. 1993. Origin of the chloride current in olfactory transduction. *Neuron* **11:**123–132

Kleene, S.J. 1994. Inhibition of olfactory cyclic nucleotide-activated current by calmodulin antagonists. *Br. J. Pharmacol* **111:**469–472

Kramer, R.H., Siegelbaum, S.A. 1992. Intracellular Ca^{2+} regulates the sensitivity of cyclic nucleotide-gated channels in olfactory receptor neurons. *Neuron* **9:**897–906

Kurahashi, T., Shibuya, T. 1990. Ca^{2+}-dependent adaptive properties in the solitary olfactory receptor cell in the newt. *Brain Res* **515:**261–268

Kurahashi, T., Yau, K.W. 1992. Co-existence of cationic and chloride components in odorant-induced current of vertebrate olfactory receptor cells. *Nature* **363:**71–74

Liu, M., Chen, T.Y., Ahamed, B., Li, J., Yau, K.W. 1994. Calcium-calmodulin modulation of the olfactory cyclic nucleotide-gated cation channel. *Science* **266:**1348–1354

Llinàs, R., Sugimori, M., Silver, R.B. 1992. Microdomains of high calcium concentration in a presynaptic terminal. *Science* **256:**677–679

Lowe, G., Gold, G.H. 1991. The spatial distributions of odorant sensitivity and odorant-induced currents in salamander olfactory receptor cells. *J. Physiol.* **442:**147–168

Lynch, J.W., Barry, P.H. 1991. Properties of transient K^+ currents and underlying single K^+ channels in rat olfactory receptor neurons. *J. Gen. Physiol.* **97:**1043–1072

Lynch, J.W., Lindemann, B. 1994. Cyclic nucleotide-gated channels of rat olfactory receptor cells: divalent cations control the sensitivity to cAMP. *J. Gen. Physiol.* **103:**87–106

Nakamura, T., Gold, G.H. 1987. A cyclic nucleotide-gated conductance in olfactory receptor cilia. *Nature* **325:**442–444

Nakatani, K., Koutalos, Y., Yau, K.W. 1995. Ca^{2+} modulation of the cGMP-gated channel of bullfrog retinal rod photoreceptors. *J. Physiol.* **484:1:**69–76

Okhi, S., Iwamoto, U., Aimoto, S., Yazawa, M., Hikichi, K. 1993. Mg^{2+} inhibits formation of 4 Ca^{2+} Calmodulin-enzyme complex at lower Ca^{2+} concentration. *J. Biol. Chem.* **268:**12388–12392

Reed, R.R. 1992. Signalling pathways in odorant detection. *Neuron* **8:**205–209

Ronnet, G.V., Cho, H., Hester, L.D., Wood, S.F., Snyder, S.H. 1993. Odorants differentially enhance phosphoinositide turnover and adenyl cyclase in olfactory receptor neuronal cultures. *J. Neurosci.* **13:**1751–1758

Saimi, K., Ling, Y. 1995. *Paramecium* Na^+ channels activated by Ca^{2+} + calmodulin: calmodulin is the Ca^{2+} sensor in the channel gating mechanism. *J. Membrane Biol.* **144:**257–265

Smith, S.J., Augustine, G.J. 1988. Calcium ions, active zones and synaptic transmitter release. *Trends Neurosci.* **11:**458–464

Zufall, F., Shepherd, G.M., Firestein, S. 1991. Inhibition of the olfactory cyclic nucleotide-gated ion channel by intracellular calcium. *Proc. R. Soc. Lond. Ser. B.* **246:**225–230